Trajectory Design for 6-DoF Asteroid Powered Landing via Convex Optimization

Yingying Zhang(✉), Jiangchuan Huang, Yang Tian, and Hutao Cui

Harbin Institute of Technology, School of Astronautics, Harbin, China
zhangyyhit@hotmail.com, hjiangchuan@126.com,
{tianyanghit,cuiht}@hit.edu.cn

Abstract. In this paper, a trajectory design algorithm via convex optimization has been proposed for the 6-DoF asteroid powered landing problem. The main contribution is that the algorithm combines the time-optimal and the fuel-optimal trajectory optimization to give a fuel-optimal trajectory in the optimal flight time. First, two constrained nonconvex optimal control problems of the time-optimal and the fuel-optimal are proposed, then the original nonconvex continuous-time infinite dimensional problems are turned to convex discrete-time finite dimensional optimization problems through linearization and discretization of the nonlinear dynamics and the nonconvex state, control constraints. By developing the successive convexification, the final trajectory is achieved by solving a sequence of convex fuel-optimal sub-problems using the optimal flight time and the time-optimal trajectory given by solving the time-optimal optimization problem in successive manner. The validity of proposed algorithm of generating the fuel-optimal trajectory in the optimal flight time is verified through numerical simulations for landing on an irregular asteroid.

Keywords: Asteroid landing · Trajectory design · Time-optimal · Fuel-optimal · Successive convexification

1 Introduction

Landing vehicle on asteroids to obtain high resolution data and soil samples is becoming increasingly popular in recent years. In order to successfully complete the mission, the spacecraft must softly land at the intended landing site with pinpoint precision. Due to the irregular shape and high rotating speed of asteroids, as well as the communication delay from the Earth, the problem under investigation is to propose a reliable algorithm of fuel-optimal powered landing

Supported by the National Natural Science Fund of China [grant numbers 61503102, 61673057].

Q. Wu et al. (Eds.): WiSATS 2020, LNICST 358, pp. 99–115, 2021.
https://doi.org/10.1007/978-3-030-69072-4_9

trajectory design in finite time that can be rapidly computed onboard the vehicle without ground control.

The closed-loop control method for asteroid landing have been studied, including the method of tracking a predesigned cubic polynomials trajectory satisfying boundary conditions [8,9,21], the closed-loop guidance based on current state and the state of landing site [4,6,17]. Though the closed-loop control is widely used on real-time trajectory generation, the thrust constraint is not included in the control formulation. The trajectory design for asteroid landing has been posed as constrained optimal control problem, includes the indirect method and the direct method. The indirect method [5,19,20] combines the costate differential equations, the Pontryagin principle and the boundary conditions to find the optimal solution, and the method suffers from poor convergence performance. The direct method [7,10] suffers from low computation speed because the method solves the original optimal control problem by nonlinear programming (NLP). The two method are not suitable for real-time trajectory generation.

In order to improve the efficiency of trajectory optimization, the trajectory design problem is transformed into the convex optimization problem. The convex optimization problem gains the advantage of low complexity, the polynomial solution time and global convergence [14], which can be solved reliably and efficiently. The convex programming approach is first applied in powered descent guidance for Mars landing [2,3,15,16]. Especially in [15,16], the successive convexification are proposed and used for trajectory optimization of the fuel-optimal problem and free-final-time problem. The successive convexification is to solve the original non-covex optimization problem by instead solving a sequence of related convex sub-problems. In [18], convex optimization is used to rapidly generate time-optimal trajectories for asteroid landing. In [12], the successive convexification is used for fuel-optimal trajectory design for landing on irregularly shaped asteroids.

The convex optimization is well-developed and can be solved with custom solvers [11]. In this paper, we aim to propose a trajectory design algorithm that can generate a fuel-optimal trajectory in the optimal time via convex optimization. First, we formulate the time-optimal and the fuel-optimal nonconvex trajectory optimization problems, then we linearize and discretize the two problems to cast them into convex sub-problems. Lastly, we combine the time-optimal and the fuel-optimal trajectory optimization, and generate the trajectory by solving the fuel-optimal optimization problem via successive convexification using the solution of the time-optimal optimization problem solved in successive manner.

The paper is organized as follows: Sect. 2 presents the nonconvex continuous-time time-optimal and fuel-optimal trajectory optimization problems for asteroid landing, Sect. 3 presents the convexification and discretization for the two problems, and outlines the successive convexification framework, Sect. 4 presents the algorithm for generating the fuel-optimal trajectory in the optimal time and the simulation results, Sect. 5 concludes this paper.

2 Problem Formulation

2.1 The Dynamics

We consider the trajectory design problem as a optimal control problem of guiding the vehicle from the initial state to the landing site. The spacecraft is modeled as a rigid actuated by three reaction wheels and six identical thrusters rigidly mounting to its body axes with a feasible range of thrust magnitude. In order to describe the motion of the vehicle, we first define two coordinate frames: $\mathcal{F}_{\mathcal{L}}$ coordinate frame and $\mathcal{F}_{\mathcal{S}}$ coordinate frame. $\mathcal{F}_{\mathcal{L}}$ is the asteroid-fixed frame centered at the asteroid's center-of-mass $o_{\mathcal{L}}$, with its $z_{\mathcal{L}}$-axis pointing along the spin axis of the asteroid, its $x_{\mathcal{L}}$-axis pointing along the asteroid's maximum (minimum) inertial principal axis, and the $y_{\mathcal{L}}$-axis completing the right-handed system. $\mathcal{F}_{\mathcal{S}}$ is the vehicle-fixed frame centered at the vehicle's center-of-mass $o_{\mathcal{S}}$, with its $z_{\mathcal{S}}$-axis pointing along the the vehicle's maximum inertial principal axis, its $x_{\mathcal{S}}$-axis pointing along the vehicle's minimum inertial principal axis, and the $y_{\mathcal{S}}$-axis completing the right-handed system.

We assume the fuel of the vehicle depletes at a rate proportional to the magnitude of the thrust vector. Denoting the mass as $m(t)$, the control thrust as $\mathbf{T}_{\mathcal{S}}(t)$, the mass depletion is given by

$$\dot{m}(t) = -\frac{|T_{\mathcal{S},x}(t)| + |T_{\mathcal{S},y}(t)| + |T_{\mathcal{S},z}(t)|}{I_{sp} \cdot g_0} = -\frac{\|\mathbf{T}_{\mathcal{S}}(t)\|_1}{I_{sp} \cdot g_0} \tag{1}$$

where I_{sp} is the vacuum specific impulse, g_0 is the Earth's standard gravity constant.

Then we express the translational of the vehicle in the $\mathcal{F}_{\mathcal{L}}$ coordinate frame, given the position $\mathbf{r}_{\mathcal{L}}(t) \in \mathbb{R}^3$, the velocity $\mathbf{v}_{\mathcal{L}}(t) \in \mathbb{R}^3$ and the gravitation $\nabla U(\mathbf{r}) \in \mathbb{R}^3$, the translational motioncan be given by

$$\dot{\mathbf{r}}_{\mathcal{L}}(t) = \mathbf{v}_{\mathcal{L}}(t) \tag{2}$$

$$\dot{\mathbf{v}}_{\mathcal{L}}(t) = -2\boldsymbol{\omega}_e \times \mathbf{v}_{\mathcal{L}}(t) - \boldsymbol{\omega}_e \times [\boldsymbol{\omega}_e \times \mathbf{r}_{\mathcal{L}}(t)] + \frac{\mathbf{T}_{\mathcal{L}}(t)}{m} + \nabla U(\mathbf{r}) \tag{3}$$

where $\boldsymbol{\omega}_e$ and $\mathbf{T}_{\mathcal{L}}(t)$ are the rotating angular velocity vector of the asteroid and the control thrust expressed in $\mathcal{F}_{\mathcal{L}}$ coordinate frame respectively.

We use MRPs (Modified Rodrigues Parameters) $\boldsymbol{\sigma}_{\mathcal{S}/\mathcal{L}}(t) \in \mathcal{S}^3$ to describe the attitude of $\mathcal{F}_{\mathcal{L}}$ coordinate frame relative to $\mathcal{F}_{\mathcal{S}}$ coordinate frame. Given the inertia tensor$\mathbf{J} \in \mathbb{S}^3_{++}$, the angular velocity vector $\boldsymbol{\omega}_{\mathcal{S}}(t) \in \mathbb{R}^3$, the torque $\mathbf{M}_{\mathcal{S}}(t) \in \mathbb{R}^3$, the rotational motion can by given by

$$\begin{aligned} \dot{\boldsymbol{\sigma}}_{\mathcal{S}/\mathcal{L}}(t) &= \frac{1}{4}\mathbf{R}(\boldsymbol{\sigma}_{\mathcal{S}/\mathcal{L}})\boldsymbol{\omega}_{\mathcal{S}/\mathcal{L}}(t) \\ &= \frac{1}{4}\mathbf{R}(\boldsymbol{\sigma}_{\mathcal{S}/\mathcal{L}}) \left[\boldsymbol{\omega}_{\mathcal{S}}(t) - \mathbf{C}_{\mathcal{S}/\mathcal{L}}\boldsymbol{\omega}_e\right] \end{aligned} \tag{4}$$

$$\mathbf{J}\dot{\boldsymbol{\omega}}_{\mathcal{S}}(t) = \mathbf{M}_{\mathcal{S}}(t) - \boldsymbol{\omega}_{\mathcal{S}}(t) \times [\mathbf{J}\boldsymbol{\omega}_{\mathcal{S}}(t)] \tag{5}$$

In Eq. (4), $\mathbf{C}_{\mathcal{S}/\mathcal{L}} \in SO(3)$ is the direction cosine matrix describing the attitude transformation from $\mathcal{F}_{\mathcal{L}}$ coordinate frame to $\mathcal{F}_{\mathcal{S}}$ coordinate frame, $\mathbf{R}(\boldsymbol{\sigma}_{\mathcal{S}/\mathcal{L}})$ and $\mathbf{C}_{\mathcal{S}/\mathcal{L}}$ are related to $\boldsymbol{\sigma}_{\mathcal{S}/\mathcal{L}}$ through the following relation

$$\mathbf{R}(\boldsymbol{\sigma}_{\mathcal{S}/\mathcal{L}}) = \begin{bmatrix} 1+\sigma_1^2-\sigma_2^2-\sigma_3^2 & 2(\sigma_1\sigma_2-\sigma_3) & 2(\sigma_1\sigma_3+\sigma_2) \\ 2(\sigma_1\sigma_2+\sigma_3) & 1-\sigma_1^2+\sigma_2^2-\sigma_3^2 & 2(\sigma_2\sigma_3-\sigma_1) \\ 2(\sigma_1\sigma_3-\sigma_2) & 2(\sigma_2\sigma_3+\sigma_1) & 1-\sigma_1^2-\sigma_2^2+\sigma_3^2 \end{bmatrix} \tag{6}$$

$$\mathbf{C}_{\mathcal{S}/\mathcal{L}} = \mathbf{E}_3 - \frac{4\left(1-\boldsymbol{\sigma}_{\mathcal{S}/\mathcal{L}}^T\boldsymbol{\sigma}_{\mathcal{S}/\mathcal{L}}\right)\left[\boldsymbol{\sigma}_{\mathcal{S}/\mathcal{L}}\right]^{\times} - 8\left(\left[\boldsymbol{\sigma}_{\mathcal{S}/\mathcal{L}}\right]^{\times}\right)^2}{\left(1+\boldsymbol{\sigma}_{\mathcal{S}/\mathcal{L}}^T\boldsymbol{\sigma}_{\mathcal{S}/\mathcal{L}}\right)^2} \tag{7}$$

where $\boldsymbol{\sigma}_{\mathcal{S}/\mathcal{L}} = [\sigma_1,\ \sigma_2,\ \sigma_3]^T$, $[\boldsymbol{\sigma}_{\mathcal{SL}}]^{\times} = \begin{bmatrix} 0 & -\sigma_3 & \sigma_2 \\ \sigma_3 & 0 & -\sigma_1 \\ -\sigma_2 & \sigma_1 & 0 \end{bmatrix}$ is the skew-symmetric matric.

With the direction cosine matrix, we can give the relation of control thrust $\mathbf{T}_{\mathcal{L}}(t)$ and $\mathbf{T}_{\mathcal{S}}(t)$, that is

$$\mathbf{T}_{\mathcal{L}}(t) = \mathbf{C}_{\mathcal{L}/\mathcal{S}}\mathbf{T}_{\mathcal{S}}(t) = \mathbf{C}_{\mathcal{S}/\mathcal{L}}^{-1}\mathbf{T}_{\mathcal{S}}(t) = \mathbf{C}_{\mathcal{S}/\mathcal{L}}^{T}\mathbf{T}_{\mathcal{S}}(t) \tag{8}$$

2.2 The State and Control Constraints

Since the asteroid is rotating and irregular-shaped, specific constraint must be imposed to avoid undesired collisions with the asteroid. Considering the possible complex terrain around the landing site, a glide-slope constraint that restricts the vehicle to fly in a cone with a cone angle of θ can meet the requirement of avoiding collisions, then the glide-slope constraint can be given by

$$cos\theta \leq \frac{\left[\mathbf{r}_{\mathcal{L}}(t)-\mathbf{r}_{tf}\right]^T\mathbf{n}_{tf}}{\|\mathbf{r}_{\mathcal{L}}(t)-\mathbf{r}_{tf}\|} \tag{9}$$

where $\mathbf{r}_{tf}$ is the landing site position, $\mathbf{n}_{tf}$ is the normal vector pointing outside the asteroid, both of them are expressed in $\mathcal{F}_{\mathcal{L}}$ coordinate frame.

Furthermore, in order to fulfill the goal of pinpoint landing, we hope the optical camera on the vehicle can track the landing site during the landing process, therefore, a FOV constraint which keeps the landing site within the FOV (field-of view) of the vehicle is introduced. Given the FOV angle β, the installation position vector of vision sensor $\boldsymbol{\rho}_{\mathcal{S}}$, and the line-of-sight direction $\mathbf{d}_{\mathcal{S}}$, the FOV constraint can be given by

$$cos\beta \leq \frac{\left[-\mathbf{C}_{\mathcal{S}/\mathcal{L}}(\mathbf{r}_{\mathcal{L}}(t)-\mathbf{r}_{tf})-\boldsymbol{\rho}_{\mathcal{S}}\right]^T\mathbf{d}_{\mathcal{S}}}{\|-\mathbf{C}_{\mathcal{S}/\mathcal{L}}(\mathbf{r}_{\mathcal{L}}(t)-\mathbf{r}_{tf})-\boldsymbol{\rho}_{\mathcal{S}}\|\|\mathbf{d}_{\mathcal{S}}\|} \tag{10}$$

Moreover, we must keep the mass of the vehicle always remains above the dry mass m_{dry}, the mass constraint is given as

$$m_{dry} \leq m(t) \tag{11}$$

For the control constraint, the magnitude of thrust vector is constrained to lie within the interval $[T_{min}, T_{max}]$, while the magnitude of torque is constrained to less then M_{max}, thus the control can be given by

$$T_{min} \leq \|\mathbf{T}_{\mathcal{S}}(t)\|_{\infty} \leq T_{max} \tag{12}$$

$$\|\mathbf{M}_{\mathcal{S}}(t)\|_{\infty} \leq M_{max} \tag{13}$$

2.3 Problem Statement

For the trajectory design problem for asteroid powered landing, we can emphasize the problem as a nonconvex continuous-time free-final-time problem to achieve the trajectory of the optimal flight time t_f, the time-optimal cost function can be given by

$$\underset{t_f,\ \mathbf{T}_{\mathcal{S}}}{minimize}\ \ t_f \tag{14}$$

If the flight time t_f can be estimated in advance, we can emphasize the problem as a nonconvex continuous-time two-point boundary problem to achieve the fuel-optimal trajectory during the time interval $[0,\ t_f]$. Noted that the fuel consumption is the mass variation, so the fuel-optimal cost function is given by

$$\underset{\mathbf{T}_{\mathcal{S}}}{minimize} \int_0^{t_f} \alpha \|\mathbf{T}_{\mathcal{S}}(t)\|_1\ dt \tag{15}$$

where $\alpha = \frac{1}{I_{sp} \cdot g_0}$ is a constant.

Both the time-optimal optimization problem and the fuel-optimal optimization problem are subject to the dynamics in Eqs. (2–6), the state and control constraint in Eqs. (9–13), and the boundary conditions as below.

$$\mathbf{r}_{\mathcal{L}}(0) = \mathbf{r}_0,\ \mathbf{v}_{\mathcal{L}}(0) = \mathbf{v}_0,\ \boldsymbol{\sigma}_{\mathcal{S}/\mathcal{L}}(0) = \boldsymbol{\sigma}_0,\ \boldsymbol{\omega}_{\mathcal{S}}(0) = \boldsymbol{\omega}_0,\ m(0) = m_{init} \tag{16}$$

$$\mathbf{r}_{\mathcal{L}}(t_f) = \mathbf{r}_{tf},\ \mathbf{v}_{\mathcal{L}}(t_f) = \mathbf{v}_{tf},\ \boldsymbol{\sigma}_{\mathcal{S}/\mathcal{L}}(t_f) = \boldsymbol{\sigma}_{tf},\ \boldsymbol{\omega}_{\mathcal{S}}(t_f) = \boldsymbol{\omega}_{tf},\ m_{dry} \leq m(t_f) \tag{17}$$

where $[\mathbf{r}_0,\ \mathbf{v}_0,\ \boldsymbol{\sigma}_0, \boldsymbol{\omega}_0]$ is the initial state, $[\mathbf{r}_{tf},\ \mathbf{v}_{tf},\ \boldsymbol{\sigma}_{tf}, \boldsymbol{\omega}_{tf}]$ is the terminal state.

3 Convex Formulation

In the section, we develop convex formulation for the time-optimal and fuel-optimal nonconvex optimization problems. Since both the two problems are nonconvex continuous-time infinite dimensional optimization problems, we must cast the original problems into a convex discrete-time finite dimensional optimization problem through convexification and discretization, then the convex problem is used as the sub-problem solved in successive manner to draw the optimal trajectory.

3.1 Convexification

Since the non-convexity of the original problem is mainly caused by the non-linearity of dynamics and the FOV constraint, we take the way of linearization of dynamics and the FOV constraint to do convexification. First, we define the state vector $\mathbf{x}(t) = \left[\mathbf{r}_{\mathcal{L}}(t)^T,\ \mathbf{v}_{\mathcal{L}}(t)^T,\ \boldsymbol{\omega}_{\mathcal{S}}(t)^T,\ \boldsymbol{\sigma}_{\mathcal{S}/\mathcal{L}}(t)^T\right]^T \in \mathbb{R}^{12}$ and control vector $\mathbf{u}(t) = \left[\mathbf{T}_{\mathcal{S}}(t)^T,\ \mathbf{M}_{\mathcal{S}}(t)^T\right]^T \in \mathbb{R}^6$, so we the express the dynamics in Eqs. (3–6) to the as the vector-valued function by

$$\frac{d\mathbf{x}(t)}{dt} = X\left[\mathbf{x}(t), \mathbf{u}(t)\right] = \left[\dot{\mathbf{r}}_{\mathcal{L}}(t)^T,\ \dot{\mathbf{v}}_{\mathcal{L}}(t)^T,\ \dot{\boldsymbol{\omega}}_{\mathcal{S}}(t)^T, \dot{\boldsymbol{\sigma}}_{\mathcal{S}/\mathcal{L}}(t)^T\right]^T \tag{18}$$

Given a reference trajectory including the state, the control and the mass $\{\hat{\mathbf{x}}(t),\ \hat{\mathbf{u}}(t),\ \hat{m}(t)\}$, we can linearize Eq. (18) with first-order Taylor expansion directly for the fuel optimal problem. The linearized system for the fuel-optimal optimization problem can given as

$$\begin{aligned}
\dot{\mathbf{x}}(t) &= \mathbf{A}(\hat{\mathbf{x}}, \hat{\mathbf{u}})\mathbf{x}(t) + \mathbf{B}(\hat{\mathbf{x}}, \hat{\mathbf{u}})\mathbf{u}(t) + \mathbf{C}(\hat{\mathbf{x}}, \hat{\mathbf{u}}) \\
\mathbf{A}(\hat{\mathbf{x}}, \hat{\mathbf{u}}) &= \frac{\partial X\left(\mathbf{x}, \mathbf{u}\right)}{\partial \mathbf{x}}\Big|_{\hat{\mathbf{x}}, \hat{\mathbf{u}}} \in \mathbb{R}^{12\times 12} \\
\mathbf{B}(\hat{\mathbf{x}}, \hat{\mathbf{u}}) &= \frac{\partial X\left(\mathbf{x}, \mathbf{u}\right)}{\partial \mathbf{u}}\Big|_{\hat{\mathbf{x}}, \hat{\mathbf{u}}} \in \mathbb{R}^{12\times 6} \\
\mathbf{C}(\hat{\mathbf{x}}, \hat{\mathbf{u}}) &= X\left(\hat{\mathbf{x}}, \hat{\mathbf{u}}\right) - \mathbf{A}(\hat{\mathbf{x}}, \hat{\mathbf{u}})\hat{\mathbf{x}} - \mathbf{B}(\hat{\mathbf{x}}, \hat{\mathbf{u}})\hat{\mathbf{u}} \in \mathbb{R}^{12}
\end{aligned} \tag{19}$$

For the time-optimal optimization problem, since the flight time t_f is unknown, we cast Eq. (18) in terms of normalized trajectory time $\tau = \frac{t}{t_f} \in [0, 1]$. Applying the chain rule to the left side of Eq. (18), we can obtain

$$\frac{d\mathbf{x}(t)}{dt} = \frac{d\mathbf{x}(t)}{d\tau}\frac{d\tau}{dt} \tag{20}$$

We define the time dilation between τ and t as λ, where $\lambda \triangleq \frac{dt}{d\tau}$, so the Eq. (20) turns to

$$\dot{\mathbf{x}}(\tau) = \frac{d\mathbf{x}(\tau)}{d\tau} = \lambda X\left[\mathbf{x}(\tau), \mathbf{u}(\tau)\right] \tag{21}$$

Given a reference trajectory including the state, the control, the mass and the time dilation $\left\{\hat{\mathbf{x}}(t),\ \hat{\mathbf{u}}(t),\ \hat{m}(t),\ \hat{\lambda}\right\}$ for the time-optimal optimization problem, we approximate Eq. (21) by first-order Taylor expansion, the linearized dynamics for the time-optimal optimization problem can given as

$$\begin{aligned}
\dot{\mathbf{x}}(\tau) &= \mathbf{G}_{\lambda}(\tau)\lambda + \mathbf{G}_x(\tau)\mathbf{x}(\tau) + \mathbf{G}_u(\tau)\mathbf{u}(\tau) + \mathbf{G}_c(\tau) \\
\mathbf{G}_{\lambda}(\tau) &= f\left[\hat{\mathbf{x}}(\tau), \hat{\mathbf{u}}(\tau)\right] \in \mathbb{R}^{12} \\
\mathbf{G}_x(\tau) &= \hat{\lambda}\frac{\partial f\left(\mathbf{x}, \mathbf{u}\right)}{\partial \mathbf{x}}\Big|_{\hat{\mathbf{x}}(\tau), \hat{\mathbf{u}}(\tau)} \in \mathbb{R}^{12\times 12} \\
\mathbf{G}_u(\tau) &= \hat{\lambda}\frac{\partial f\left(\mathbf{x}, \mathbf{u}\right)}{\partial \mathbf{u}}\Big|_{\hat{\mathbf{x}}(\tau), \hat{\mathbf{u}}(\tau)} \in \mathbb{R}^{12\times 6} \\
\mathbf{G}_c(\tau) &= -\mathbf{G}_x(\tau)\hat{\mathbf{x}}(\tau) - \mathbf{G}_u(\tau)\hat{\mathbf{u}}(\tau) \in \mathbb{R}^{12}
\end{aligned} \tag{22}$$

By the definition of the time dilation λ, we can get $\lambda = t_f$, so the time-optimal cost function in Eq. (14) turns to

$$\underset{\lambda,\ \mathbf{T}_{\mathcal{S}}}{minimize}\ \ \lambda \tag{23}$$

For the glide-slope constraint and the FOV constraint, they can be expressed as the following equivalent form

$$\|\mathbf{C}_e\mathbf{x}(t) - \mathbf{C}_e\mathbf{x}_{tf}\| \leq \frac{\mathbf{n}_{tf}^T\mathbf{C}_e}{cos\theta}\left[\mathbf{x}(t) - \mathbf{x}_{tf}\right] \tag{24}$$

$$\|\mathbf{C}_{\mathcal{S}/\mathcal{L}}\mathbf{C}_e(\mathbf{r}(t) - \mathbf{r}_{tf}) + \boldsymbol{\rho}_{\mathcal{S}}\| + \frac{\mathbf{d}_{\mathcal{S}}^T}{cos\beta\|\mathbf{d}_{\mathcal{S}}\|}\left[\mathbf{C}_{\mathcal{S}/\mathcal{L}}\mathbf{C}_e(\mathbf{r}(t) - \mathbf{r}_{tf}) + \boldsymbol{\rho}_{\mathcal{S}}\right] \leq 0 \tag{25}$$

where $\mathbf{C}_e = [\mathbf{E}_3,\ \mathbf{0}_{3\times 9}] \in \mathbb{R}^{3\times 12}$, $\mathbf{x}_{tf} = \left[\mathbf{r}_{tf}^T,\ \mathbf{v}_{tf}^T,\ \boldsymbol{\sigma}_{tf}^T, \boldsymbol{\omega}_{tf}^T\right]^T$ is the terminal state.

For the fuel-optimal optimization problem, the glide-slope constraint in Eq. (24) is in the convex form of second-order cone, but the FOV constraint in Eq. (25) is nonlinear, so we linearize the left side of Eq. (25) by first-order Taylor expansion to make it convex, that we have

$$q\left(\hat{\mathbf{x}}\right)'\mathbf{x}(t) + q\left(\hat{\mathbf{x}}\right) - q\left(\hat{\mathbf{x}}\right)'\hat{\mathbf{x}}(t) \leq 0 \tag{26}$$

$$\begin{aligned}
q\left(\mathbf{x}\right) &= \|f(\mathbf{x})\| + \frac{\mathbf{d}_{\mathcal{S}}^T}{cos\beta\|\mathbf{d}_{\mathcal{S}}\|}f(\mathbf{x}) \in \mathbb{R} \\
q\left(\mathbf{x}\right)' &= \frac{f\left(\mathbf{x}\right)^T}{\|f(\mathbf{x})\|}f(\mathbf{x})' + \frac{\mathbf{d}_{\mathcal{S}}^T}{cos\beta\|\mathbf{d}_{\mathcal{S}}\|}f(\mathbf{x})' \in \mathbb{R}^{1\times 12} \\
f\left(\mathbf{x}\right) &= \mathbf{C}_{\mathcal{S}/\mathcal{L}}\mathbf{C}_e\mathbf{x}(t) - \mathbf{C}_{\mathcal{S}/\mathcal{L}}\mathbf{C}_e\mathbf{x}_{tf} + \boldsymbol{\rho}_{\mathcal{S}} \in \mathbb{R}^3 \\
f\left(\mathbf{x}\right)' &= \mathbf{C}_{\mathcal{S}/\mathcal{L}}\mathbf{C}_e + \frac{\partial\left[\mathbf{C}_{\mathcal{S}/\mathcal{L}}\mathbf{C}_e\mathbf{x}(t)\right]}{\partial\boldsymbol{\sigma}}\mathbf{C}_{\sigma} \in \mathbb{R}^{3\times 12}
\end{aligned}$$

where $\mathbf{C}_{\sigma} = [\mathbf{0}_{3\times 9},\ \mathbf{E}_3] \in \mathbb{R}^{3\times 12}$.

For the time-optimal optimization problem, the glide-slope constraint and FOV constraint share the same form in Eqs. (25) and (26), we just need replace t with τ.

For the control constraint, the left side of Eq. (12) $T_{min} \leq \|\mathbf{T}_{\mathcal{S}}(t)\|_{\infty}$ is nonconvex. Given $\hat{\mathbf{T}}_{\mathcal{S}}(t) \in \hat{\mathbf{u}}(t)$, we can use the following convex relation for the thrust constraint.

$$T_{min} \leq \frac{\hat{T}_{\mathcal{S},j}(t)}{|\hat{T}_{\mathcal{S},j}(t)|}T_{\mathcal{S},j}(t) \leq T_{max} \quad j = x, y, z \tag{27}$$

where $\mathbf{T}_{\mathcal{S}}(t) = [T_{\mathcal{S},x}(t),\ T_{\mathcal{S},y}(t), T_{\mathcal{S},z}(t)]^T$.

3.2 Successive Convexification

After convexification for the original problems, they have been turned to convex optimization problems. The convex problem can be regarded as a sub-problem solved in successive convexification process, so we can we indirectly solve the original nonconvex optimization problems by instead solving a sequence of related convex sub-problems, and the sub-problem in each iteration can be solved by second-order cone programming. First, we do discretization for the time-optimal and the fuel-optimal convex optimization problems.

For the fuel-optimal optimization problem, we discretize the time domain $t \in [0,\ t_f]$ into N equal intervals with the time increment Δt, the temporal nodes are

$$t_k = k\Delta t,\ k = 0, 1, 2, ..., N \tag{28}$$

We conduct the zero-order-hold control in each discrete time interval, and denote $\mathbf{x}(k) = \mathbf{x}(t_k)$, $\mathbf{u}(k) = \mathbf{u}(t_k)$, $m(k) = m(t_k)$. Denoting the i^{th} iteration in the successive convexification by superscript i, we replace the reference trajectory $\{\hat{\mathbf{x}}(t),\ \hat{\mathbf{u}}(t),\ \hat{m}(t)\}$ with $i-1^{th}$ successive solution $\left\{\mathbf{x}^{i-1}(k),\ \mathbf{u}^{i-1}(k),\ m^{i-1}(k)\right\}$, then the discrete-time mass depletion and dynamics for the fuel-optimal optimization problem can be given by

$$m^{i-1}(k+1) = m^{i-1}(k) - \alpha\|\mathbf{T}_{\mathcal{S}}^{i-1}(k)\|_1\Delta t \tag{29}$$

$$\mathbf{x}^i(k+1) = \bar{\mathbf{A}}^i(k)\mathbf{x}^i(k) + \bar{\mathbf{B}}^i(k)\mathbf{u}^i(k) + \bar{\mathbf{C}}^i(k) \tag{30}$$

$$\begin{aligned}
\bar{\mathbf{A}}^i(k) &= \phi_A(\Delta t) = e^{\Delta t\mathbf{A}(\mathbf{x}^{i-1},\mathbf{u}^{i-1})} \\
\bar{\mathbf{B}}^i(k) &= \int_0^{\Delta t} \phi_A(\Delta t - \xi)\mathbf{B}(\mathbf{x}^{i-1},\mathbf{u}^{i-1})\,d\xi \\
\bar{\mathbf{C}}^i(k) &= \int_0^{\Delta t} \phi_A(\Delta t - \xi)\mathbf{C}(\mathbf{x}^{i-1},\mathbf{u}^{i-1})\,d\xi
\end{aligned}$$

The discretized cost function for the fuel-optimal optimaization problem turns to

$$\underset{\mathbf{T}_{\mathcal{S}}}{minimize} \sum_{k=0}^{N-1} \alpha\|\mathbf{T}_{\mathcal{S}}^i(k)\|_1\Delta t \tag{31}$$

For the time-optimal optimization problem, we discretize the normalized time domain $\tau \in [0,\ 1]$ into N equal intervals, the temporal nodes are

$$\tau_k = \frac{k}{N},\ k = 0, 1, 2, ..., N \tag{32}$$

Denoting $\mathbf{x}(k) = \mathbf{x}(\tau_k)$, $\mathbf{u}(k) = \mathbf{u}(\tau_k)$ and $m(k) = m(\tau_k)$, and replacing the reference trajectory $\left\{\hat{\mathbf{x}}(t),\ \hat{\mathbf{u}}(t),\ \hat{m}(t),\ \hat{\lambda}\right\}$ with $\left\{\mathbf{x}^{i-1}(k), \mathbf{u}^{i-1}(k), m^{i-1}(k), \lambda^{i-1}\right\}$, the discrete-time mass depletion dynamics for the time-optimal optimization problem can be given by

$$m^{i-1}(k+1) = m^{i-1}(k) - \frac{\lambda^{i-1}}{N}\alpha\|\mathbf{T}_{\mathcal{S}}^{i-1}(k)\|_1 \tag{33}$$

$$\begin{aligned}
\mathbf{x}^i(k+1) &= \bar{\mathbf{G}}_x^i(k)\mathbf{x}^i(k) + \bar{\mathbf{G}}_u^i(k)\mathbf{u}^i(k) + \bar{\mathbf{G}}_\lambda^i(k)\lambda^i + \bar{\mathbf{G}}_c^i(k) \qquad (34)\\
\bar{\mathbf{G}}_x^i(k) &= \bar{\phi}(\tau_{k+1}-\tau_k) = e^{(\tau_{k+1}-\tau_k)\mathbf{G}_x^{i-1}(k)}\\
\bar{\mathbf{G}}_u^i(k) &= \int_{\tau_k}^{\tau_{k+1}} \bar{\phi}(\tau_{k+1}-\xi)G_u^{i-1}(k)\ d\xi\\
\bar{\mathbf{G}}_\lambda^i(k) &= \int_{\tau_k}^{\tau_{k+1}} \bar{\phi}(\tau_{k+1}-\xi)G_\lambda^{i-1}(k)\ d\xi\\
\bar{\mathbf{G}}_c^i(k) &= \int_{\tau_k}^{\tau_{k+1}} \bar{\phi}(\tau_{k+1}-\xi)G_c^{i-1}(k)\ d\xi
\end{aligned}$$

The discrete-time state constraints and control constraints for both the fuel-optimal and the time-optimal optimization problems share the following relation.

$$\|\mathbf{C}_e\mathbf{x}^i(k) - \mathbf{C}_e\mathbf{x}^i(N)\| \leq \frac{\mathbf{n}_{tf}^T\mathbf{C}_e}{cos\theta}\left[\mathbf{x}^i(k) - \mathbf{x}^i(N)\right] \qquad (35)$$

$$q\left[\mathbf{x}^{i-1}(k)\right]'\mathbf{x}^i(k) + q\left[\mathbf{x}^{i-1}(k)\right] - q\left[\mathbf{x}^{i-1}(k)\right]'\mathbf{x}^{i-1}(k) \leq 0 \qquad (36)$$

$$T_{min} \leq \frac{T_{\mathcal{S},j}^{i-1}(k)}{|T_{\mathcal{S},j}^{i-1}(k)|}T_{\mathcal{S},j}^i(k) \leq T_{max} \quad j = x, y, z \qquad (37)$$

$$\|\mathbf{M}_{\mathcal{S}}^i(k)\|_\infty \leq M_{max} \qquad (38)$$

where $\mathbf{x}^i(N)$ is the terminal state.

In addition, in order to make the successive convexification work, we must ensure that the problem remains bounded and feasible throughout sequence iteration. Therefore, we introduce virtual control and trust regions.

The virtual control is used to eliminate the artificial infeasibility caussed by the linearization for the dynamics and the FOV constraint, we augment virtual control $\mathbf{V}_x^i(k) \in \mathbb{R}^{12}$ and $V_f^i(k) \in \mathbb{R}_+$ to the dynamics in Eqs. (30, 34) and constrains in Eq. (36), we can obtain

$$\mathbf{x}^i(k+1) = \bar{\mathbf{A}}^i(k)\mathbf{x}^i(k) + \bar{\mathbf{B}}^i(k)\mathbf{u}^i(k) + \bar{\mathbf{C}}^i(k) + \mathbf{V}_x^i(k) \qquad (39)$$

$$\mathbf{x}^i(k+1) = \bar{\mathbf{G}}_x^i(k)\mathbf{x}^i(k) + \bar{\mathbf{G}}_u^i(k)\mathbf{u}^i(k) + \bar{\mathbf{G}}_\lambda^i(k)\lambda^i + \bar{\mathbf{G}}_c^i(k) + \mathbf{V}_x^i(k) \qquad (40)$$

$$q\left[\mathbf{x}^{i-1}(k)\right]'\mathbf{x}^i(k) + q\left[\mathbf{x}^{i-1}(k)\right] - q\left[\mathbf{x}^{i-1}(k)\right]'\mathbf{x}^{i-1}(k) \leq V_f^i(k), \quad V_f^i(k) \geq 0 \qquad (41)$$

The trust regions is to ensure the linearization can capture the nonlinearity of the original problems and keep the problem remain bounded, which make the trajectory not significantly deviate from the previous iteration. To do so, we first define the state deviation between the i^{th} iteration and the $i-1^{th}$ iteration as

$$\delta\mathbf{x}_k^i = \mathbf{x}^i(k) - \mathbf{x}^{i-1}(k) \qquad (42)$$

Then we introduce the following constraint

$$\left[\delta\mathbf{x}_k^i\right]^T\delta\mathbf{x}_k^i \leq \Delta_k^i \qquad (43)$$

where $\Delta_k^i \in \mathbb{R}_+$ is the square of the trust region radius, the corresponding trust region center is located at $\mathbf{x}^{i-1}(k)$.

Adding the penalty term about trust regions and virtual control to the cost function in Eq. (23) and (31), we can obtain

$$\underset{\lambda,\ \mathbf{T}}{minimize}\ \ J^i[\lambda] = \lambda^i + W_x\|\mathbf{V}_x^i\|_1 + W_f\|\mathbf{V}_f^i\|_1 + W_\Delta\|\boldsymbol{\Delta}^i\|_1 \tag{44}$$

$$\underset{\mathbf{T}}{minimize}\ J^i[\mathbf{T}(k)] = \alpha\|\mathbf{T}^i\|_1\Delta t + W_x\|\mathbf{V}_x^i\|_1 + W_f\|\mathbf{V}_f^i\|_1 + W_\Delta\|\boldsymbol{\Delta}^i\|_1 \tag{45}$$

where $\mathbf{T}^i = \left[\mathbf{T}_{\mathcal{S}}^i(0)^T, \ldots, \mathbf{T}_{\mathcal{S}}^i(N-1)^T\right]^T$, $\mathbf{V}_x^i = \left[\mathbf{V}_x^i(0)^T, \ldots, \mathbf{V}_x^i(N-1)^T\right]^T$, and $\mathbf{V}_f^i = \left[V_f^i(0)\ , \ldots, V_f^i(N)\right]^T$, $\boldsymbol{\Delta}^i = \left[\Delta_0^i\ , \ldots, \Delta_k^i\ , \ldots, \Delta_N^i\right]^T$, W_x and W_f are the weight for virtual controls, W_Δ is the weight for the trust region.

3.3 Convex Sub-problem

In this section, we summarize the convex sub-problem which is solved repeatedly by the successive convexification method for the time-optimal and the fuel-optimal optimization problems. The summary of the convex subproblem is provided as below.

Problem 1. Convex discrete-time time-optimal convex optimization subproblem

$$\underset{\lambda,\ \mathbf{T}}{minimize}\ \ J^i[\lambda] = \lambda^i + W_x\|\mathbf{V}_x^i\|_1 + W_f\|\mathbf{V}_f^i\|_1 + W_\Delta\|\boldsymbol{\Delta}^i\|_1$$

subject to

$$m^{i-1}(k+1) = m^{i-1}(k) - \frac{\lambda^{i-1}}{N}\alpha\|\mathbf{T}_{\mathcal{S}}^{i-1}(k)\|_1$$

$$\mathbf{x}^i(k+1) = \bar{\mathbf{G}}_x^i(k)\mathbf{x}^i(k) + \bar{\mathbf{G}}_u^i(k)\mathbf{u}^i(k) + \bar{\mathbf{G}}_\lambda^i(k)\lambda^i + \bar{\mathbf{G}}_c^i(k) + \mathbf{V}_x^i(k)$$

$$\|\mathbf{C}_e\mathbf{x}^i(k) - \mathbf{C}_e\mathbf{x}^i(N)\| \le \frac{\mathbf{n}_{tf}^T\mathbf{C}_e}{cos\theta}\left[\mathbf{x}^i(k) - \mathbf{x}^i(N)\right]$$

$$q\left[\mathbf{x}^{i-1}(k)\right]'\mathbf{x}^i(k) + q\left[\mathbf{x}^{i-1}(k)\right] - q\left[\mathbf{x}^{i-1}(k)\right]'\mathbf{x}^{i-1}(k) \le V_f^i(k), \quad V_f^i(k) \ge 0$$

$$\left[\delta\mathbf{x}_k^i\right]^T\delta\mathbf{x}_k^i \le \Delta_k^i \qquad \|\mathbf{M}_{\mathcal{S}}^i(k)\|_\infty \le M_{max}$$

$$T_{min} \le \frac{T_{\mathcal{S},j}^{i-1}(k)}{|T_{\mathcal{S},j}^{i-1}(k)|}T_{\mathcal{S},j}^i(k) \le T_{max} \quad j = x, y, z$$

$$m^i(0) = m_{init} \quad \mathbf{x}^i(0) = \left[\mathbf{r}_0^T,\ \mathbf{v}_0^T,\ \boldsymbol{\omega}_0^T,\ \boldsymbol{\sigma}_0^T\right]^T \tag{46}$$

$$m_{dry} \le m^i(N) \quad \mathbf{x}^i(N) = \left[\mathbf{r}_{tf}^T,\ \mathbf{v}_{tf}^T,\ \boldsymbol{\omega}_{tf}^T,\ \boldsymbol{\sigma}_{tf}^T\right]^T \tag{47}$$

Problem 2. Convex discrete-time fuel-optimal convex optimization subproblem

$$\underset{\mathbf{T}}{minimize}\ J^i[\mathbf{T}(k)] = \alpha\|\mathbf{T}^i\|_1\Delta t + W_x\|\mathbf{V}_x^i\|_1 + W_f\|\mathbf{V}_f^i\|_1 + W_\Delta\|\boldsymbol{\Delta}^i\|_1$$

subject to

$$m^{i-1}(k+1) = m^{i-1}(k) - \alpha \|\mathbf{T}_{\mathcal{S}}^{i-1}(k)\|_1 \Delta t$$

$$\mathbf{x}^i(k+1) = \bar{\mathbf{A}}^i(k)\mathbf{x}^i(k) + \bar{\mathbf{B}}^i(k)\mathbf{u}^i(k) + \bar{\mathbf{C}}^i(k) + \mathbf{V}_x^i(k)$$

$$\|\mathbf{C}_e\mathbf{x}^i(k) - \mathbf{C}_e\mathbf{x}^i(N)\| \leq \frac{\mathbf{n}_{tf}^T\mathbf{C}_e}{cos\theta}\left[\mathbf{x}^i(k) - \mathbf{x}^i(N)\right]$$

$$q\left[\mathbf{x}^{i-1}(k)\right]'\mathbf{x}^i(k) + q\left[\mathbf{x}^{i-1}(k)\right] - q\left[\mathbf{x}^{i-1}(k)\right]'\mathbf{x}^{i-1}(k) \leq V_f^i(k), \quad V_f^i(k) \geq 0$$

$$\left[\delta\mathbf{x}_k^i\right]^T \delta\mathbf{x}_k^i \leq \Delta_k^i \qquad \|\mathbf{M}_{\mathcal{S}}^i(k)\|_\infty \leq M_{max}$$

$$T_{min} \leq \frac{T_{\mathcal{S},j}^{i-1}(k)}{|T_{\mathcal{S},j}^{i-1}(k)|} T_{\mathcal{S},j}^i(k) \leq T_{max} \quad j = x, y, z$$

$$m^i(0) = m_{init} \quad \mathbf{x}^i(0) = \left[\mathbf{r}_0^T,\ \mathbf{v}_0^T,\ \boldsymbol{\omega}_0^T,\ \boldsymbol{\sigma}_0^T\right]^T$$

$$m_{dry} \leq m^i(N) \quad \mathbf{x}^i(N) = \left[\mathbf{r}_{tf}^T,\ \mathbf{v}_{tf}^T,\ \boldsymbol{\omega}_{tf}^T,\ \boldsymbol{\sigma}_{tf}^T\right]^T$$

where Eqs. (46) and (47) are the discrete boundary condition to be enforced in each iteration.

3.4 Algorithm

In this paper, we propose two problems, the time-optimal convex optimization problem and the fuel-optimal optimization problem. The fuel-optimal optimization problem is assumed to be a fixed flight time optimization problem, that means the algorithm should determine the optimal flight time t_f which yields minimum fuel consumption over the landing process. The algorithm for solving the time-optimal optimization problem can provide the estimation of the optimal flight time, so we combine the time-optimal optimization and the fuel-optimal optimization for trajectory design. First, we solve the convex discrete-time time-optimal optimization sub-problem (Problem 1) in the successive manner to give the optimal flight time λ and the time-optimal trajectory. The flight time for the fuel-optimal optimization problem is $t_f = \lambda$. Making the obtained time-optimal trajectory as the initial reference trajectory, then the fuel-optimal trajectory is achieved by solving the convex discrete-time fuel-optimal convex optimization sub-problem (Problem 2) through successive convexification. The algorithm is shown in Algorithm 1.

Algorithm 1. Algorithm for asteroid landing trajectory design

(i) **Initialization**

Input the vehicle parameters, the initial condition $\left[\mathbf{r}_0^T,\ \mathbf{v}_0^T,\ \boldsymbol{\omega}_0^T,\ \boldsymbol{\sigma}_0^T\right]^T$ and the terminal condition $\left[\mathbf{r}_{tf}^T,\ \mathbf{v}_{tf}^T,\ \boldsymbol{\omega}_{tf}^T,\ \boldsymbol{\sigma}_{tf}^T\right]^T$, the initial reference trajectory $\{\mathbf{x}^0(k), \mathbf{u}^0(k), m^0(k), \lambda^0\}$, the maximum iteration number N_{iter} and an acceptable state trajectory deviation ε_x.

(ii) **Successive Optimization Loop**

a) Calculate the coefficient matrices $\bar{\mathbf{G}}_x^0(k)$, $\bar{\mathbf{G}}_u^0(k)$, $\bar{\mathbf{G}}_\lambda^0(k)$, $\bar{\mathbf{G}}_c^0(k)$, $q\left[\mathbf{x}^0(k)\right]'$, $q\left[\mathbf{x}^0(k)\right]$ by using Eqs. (22, 26, 34), then compute $\mathbf{x}^1(k)$ and all the state constraints that $\mathbf{x}^1(k)$ needs to satisfy in Eqs. (35, 37, 38, 40, 41) with $\{\mathbf{x}^0(k), \mathbf{u}^0(k), m^0(k), \lambda^0\}$.

If $i \leq N_{iter}$ $(i \geq 1)$

If $\|\delta \mathbf{x}^i\|_\infty \geq \varepsilon_x$

(1) solve Problem 1 and compute $J^i[\lambda]$ by convex optimization

(2) store the successive solution $\{\mathbf{x}^i(k), \mathbf{u}^i(k), \lambda\}$ compute $m^i(k)$ by using Eq. (33).

(3) make $\mathbf{x}^i(k)$, $\mathbf{u}^i(k)$, $m^i(k)$, λ^i be the new reference trajectory $\hat{\mathbf{x}}(t)$, $\hat{\mathbf{u}}(t)$, $\hat{m}(t)$, $\hat{\lambda}$, then calculate the coefficient matrices $\bar{\mathbf{G}}_x^i(k)$, $\bar{\mathbf{G}}_u^i(k)$, $\bar{\mathbf{G}}_\lambda^i(k)$, $\bar{\mathbf{G}}_c^i(k)$, $q\left[\mathbf{x}^i(k)\right]'$, $q\left[\mathbf{x}^i(k)\right]$ by using Eqs. (22, 26, 34), and give $\mathbf{x}^{i+1}(k)$ and all the state constraints that $\mathbf{x}^{i+1}(k)$ needs to satisfy in Eqs. (35, 37, 38, 40, 41).

(4) return step (1) to compute $J^i[\lambda]$ and solve Problem 1.

else

Stop and compute $m^i(k)$, store $\{\mathbf{x}^i(k), \mathbf{u}^i(k), m^i(k), \lambda^i\}$

end

end

b) Make $t_f = \lambda^i$, calculate the coefficient matrices $\bar{\mathbf{A}}^0(k)$, $\bar{\mathbf{B}}^0(k)$, $\bar{\mathbf{C}}^i(k)$, $q\left[\mathbf{x}^0(k)\right]'$, $q\left[\mathbf{x}^0(k)\right]$ by using Eqs. (19, 26, 30), then compute $\mathbf{x}^1(k)$ and all the state constraints that $\mathbf{x}^1(k)$ needs to satisfy in Eqs. (35, 37–39, 41) with $\{\mathbf{x}^i(k), \mathbf{u}^i(k), m^i(k)\}$.

If $j \leq N_{iter}$ $(j \geq 1)$

If $\|\delta \mathbf{x}^j\|_\infty \geq \varepsilon_x$

(1) solve Problem 2 and compute $J^j[\mathbf{T}(k)]$ by convex optimization

(2) store the successive solution $\{\mathbf{x}^j(k), \mathbf{u}^j(k)\}$ and compute $m^j(k)$ by using Eq. (29).

(3) let $\mathbf{x}^j(k)$, $\mathbf{u}^j(k)$ and $m^j(k)$ be the new reference trajectory $\hat{\mathbf{x}}(k)$, $\hat{\mathbf{u}}(k)$ and $\hat{m}(k)$, then calculate the coefficient matrices $\bar{\mathbf{A}}^j(k)$, $\bar{\mathbf{B}}^j(k)$, $\bar{\mathbf{C}}^j(k)$, $q\left[\mathbf{x}^j(k)\right]'$, $q\left[\mathbf{x}^j(k)\right]$ by using Eqs. (19, 26, 30), and give $\mathbf{x}^{j+1}(k)$ and all the state constraints that $\mathbf{x}^{j+1}(k)$ needs to satisfy in Eqs. (35, 37–39, 41).

(4) return step (1) to compute $J^j[\mathbf{T}(k)]$ and solve Problem 2.

else

Stop and compute $m^j(k)$, output $\{\mathbf{x}^j(k), \mathbf{u}^j(k), m^j(k)\}$

end

end

4 Simulation Results

In this section, we present simulation results to examine our algorithm. The simulation is carried in MATLAB software using convex programming (CVX) and the solver SDPT3 4.0. We study the trajectory landing on asteroid 4769 Castalia. The diameter and density for the asteroid are 1.4 km and 2100 kg/m^3, the rotation period is 4.095 h, the GM is 94 m^3/s^2. The polyhedron gravitation method [13] is adopted to calculate the asteroid gravity using a shape model with 2048 vertices and 4092 faces the shape model data can be downloaded from [1]. The parameters for the vehicle are given in Table 1.

Table 1. The vehicle parameters

Parameters	Values
Initial moment of inertia	$\mathbf{J} = \begin{bmatrix} 2940 & 0 & 0 \\ 0 & 2758 & 0 \\ 0 & 0 & 1974 \end{bmatrix}$ kg · m^2
Mass of vehicle	$m_{init} = 1400$ kg $\quad m_{dry} = 1000$ kg
Thrust and Torque	$T_{min} = 2$ N $\quad T_{max} = 20$ N $\quad M_{max} = 0.2$ Nm
Vision sensor parameters	$\boldsymbol{\rho}_{\mathcal{S}} = [0.9,\ 0,\ -1.0]^T \quad \mathbf{d}_{\mathcal{S}} = [0,\ 0,\ -1.0]^T$ $\beta = 25$ deg
Glide-slope	$\theta = 15$ deg
Vacuum specific impulse	$I_{sp} = 225$ s
Earth's standard gravity constant	$g_0 = 9.80665$ m/s^2

To start the successive convexification, we first do a simulation of the time-optimal convex sub-problem just considering the dynamics and convex control constraints with a reference state $\mathbf{x}_k^0 = \frac{N-k}{N}\mathbf{x}_0 + \frac{k}{N}\mathbf{x}_f,\ k = 0, 1, ..., N$, and use the obtained solution as the initial reference trajectory $\{\mathbf{x}^0(k), \mathbf{u}^0(k), m^0(k), \lambda^0\}$. The initial state and terminal state for the vehicle are given as follows.

$$\mathbf{r}_0 = [-237.554,\ -7.151,\ 1255.3]^T\ m \quad \mathbf{v}_0 = [1.423,\ 1.376,\ 0.698]^T\ m/s$$
$$\boldsymbol{\omega}_0 = [0,\ 0,\ 0]^T\ rad/s \qquad \boldsymbol{\sigma}_0 = [0.1004,\ 0.0111,\ -0.3537]^T$$
$$\mathbf{r}_{tf} = [0,\ 0,\ 289.3730]^T\ m \qquad \mathbf{v}_{tf} = [0,\ 0,\ 0]^T\ m/s$$
$$\boldsymbol{\omega}_{tf} = [0.0001,\ 0.0001,\ 0.0005]^T\ rad/s\ \boldsymbol{\sigma}_{tf} = [0.0882,\ -0.0784,\ -0.3791]^T$$

Given the acceptable state trajectory deviation ε_x, when $\|\delta\mathbf{x}_k^i\|_\infty \leq \varepsilon_x$, the sequence iteration stops, and the solution of the last iteration is the optimal trajectory. We set $\varepsilon_x = 10^{-3}$, the simulation results of state and control, angle of glide-slope and FOV, mass depletion and the trajectories for the time-optimal optimization problem and the fuel-optimal optimization problem (using the simulation results of the time-optimal problem as the initial reference trajectory and the flight time) are given in Figs. 1, 2, 3, 4, 5, 6, 7, 8, 9 and 10.

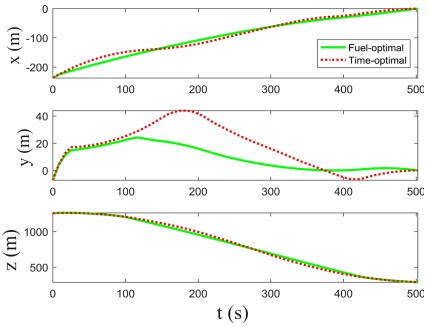

Fig. 1. The position $\mathbf{r}_{\mathcal{L}}$

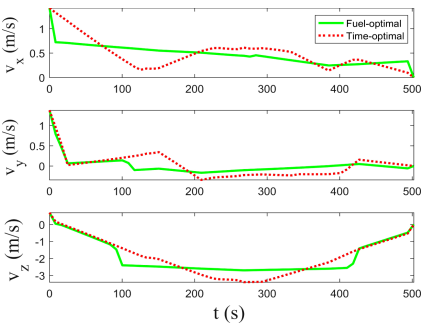

Fig. 2. The velocity $\mathbf{v}_{\mathcal{L}}$

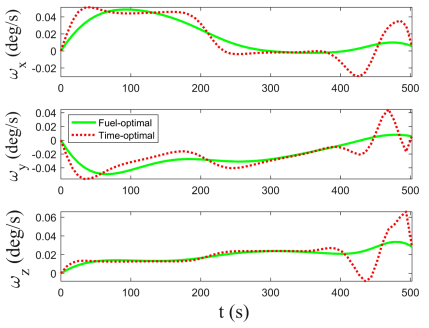

Fig. 3. The angular velocity $\boldsymbol{\omega}_{\mathcal{S}}$

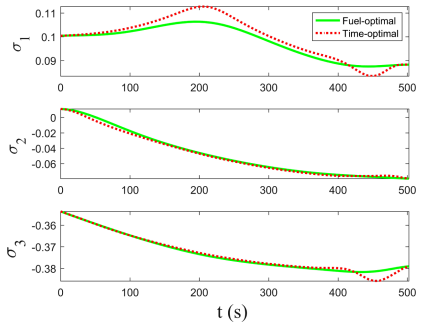

Fig. 4. The MRPs $\boldsymbol{\sigma}_{\mathcal{S}/\mathcal{L}}$

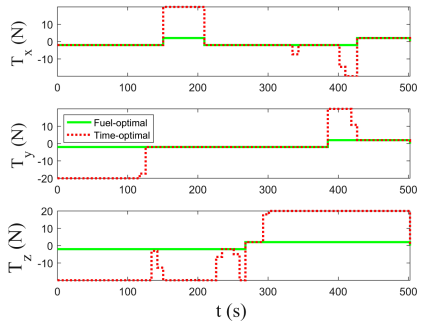

Fig. 5. The thrust $\mathbf{T}_{\mathcal{S}}$

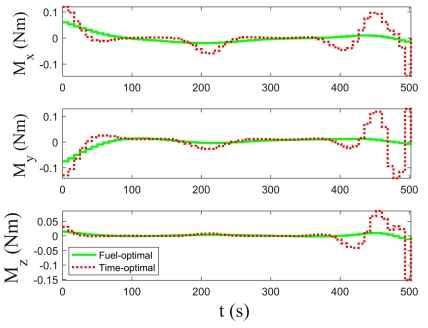

Fig. 6. The torque $\mathbf{M}_{\mathcal{S}}$

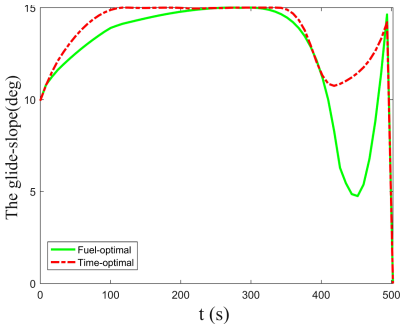

Fig. 7. The angle of the glide-slope

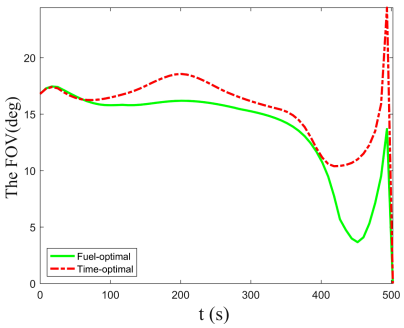

Fig. 8. The angle of the FOV

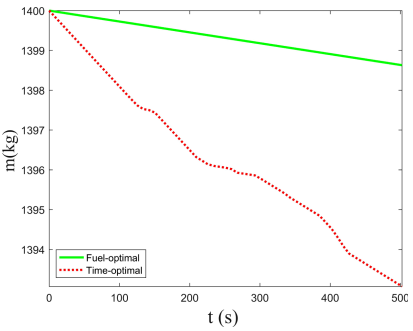

Fig. 9. The mass depletion

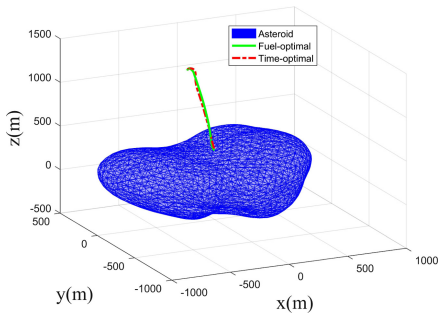

Fig. 10. The trajectory for landing on asteroid

For solving time-optimal optimization problem, the time dilation is $\lambda = 502.1388$, the iteration number is 7, the cut-off state deviation $\|\delta \mathbf{x}_k^i\|_\infty$ is 4.0920×10^{-6}, the CPU time is $78.1218s$. Making $t_f = \lambda$ and using the obtained time-optimal trajectory as the initial reference trajectory for solving fuel-optimal optimization problem, the iteration number is 4, the cut-off state deviation $\|\delta \mathbf{x}_k^i\|_\infty$ is 1.5202×10^{-4}, the CPU time is $56.4646s$, and the fuel-optimal optimization problem uses less fuel to obtain a more stable trajectory than that of the time-optimal optimization problem as can be seen from Figs. (1-10), the fuel consumption for the time-optimal optimization problem is $6.9303kg$ while the fuel consumption for the fuel-consumption optimization problem is $1.3654kg$. The simulation results indicate that the trajectory design algorithm combining the time-optimal and the fuel-optimal optimization problems solved by successive convexifcation is feasible and reliable, the calculation speed is relatively fast, which can be extended to onboard real-time calculation.

5 Conclusions

In this paper, a trajectory design algorithm via convex optimization has been proposed to solve the problem of 6-DoF asteroid powered landing. The asteroid landing problem is reformulated as a constrained optimal control problem, with the nonlinear translational and rotational dynamics, the nonconvex state and control constraints. Two optimization problems of the time-optimal and fuel-optimal are considered, through linearization and discretization of nonlinear dynamics and nonconvex constraints, the nonlinearity and dimension of the original problems are reduced, then successive convexification is developed to solve the two optimization problems. In the algorithm, the trajectory design combines the time-optimal and the fuel-optimal trajectory optimization, the trajectory is given by solving the fuel-optimal optimization problem via successive convexification using the flight time and time-optimal trajectory obtained by solving the time-optimal optimization problem in successive manner. Simulations are conducted in order to examine the proposed algorithm. The simulation results indicate that the trajectory design algorithm is capable of generating optimal solutions (the fuel-optimal trajectory in the optimal flight time) for asteroid powered landing with relatively fast computational speed. Consequently, the proposed algorithm can be extended to onboard applications.

References

1. NASA PDS: Small Bodies Node, 31 January 2019. https://pdssbn.astro.umd.edu/
2. Acikmese, B., Ploen, S.R.: Convex programming approach to powered descent guidance for mars landing. J. Guid. Control Dyn. **30**(5), 1353–1366 (2007). https://doi.org/10.2514/1.27553
3. Blackmore, L., Acikmese, B., Scharf, D.P.: Minimum-landing-error powered-descent guidance for mars landing using convex optimization. J. Guid. Control Dyn. **33**(4), 1161–1171 (2010). https://doi.org/10.2514/1.47202
4. Furfaro, R., Cersosimo, D., Wibben, D.R.: Asteroid precision landing via multiple sliding surfaces guidance techniques. J. Guid. Control Dyn. **36**(4), 1075–1092 (2013). https://doi.org/10.2514/1.58246
5. Gregory, L., Robert, B.: Optimal trajectories for soft landing on asteroids. Space Systems Design Lab., Georgia Inst. of Technology, AE8900 MS Special Problems Report (2017)
6. Hawkins, M., Guo, Y., Wie, B.: Zem/zev feedback guidance application to fuel-efficient orbital maneuvers around an irregular-shaped asteroid. In: AIAA Guidance, Navigation, and Control Conference, p. 5045 (2012), https://doi.org/10.2514/6.2012-5045
7. Hu, H., Zhu, S., Cui, P.: Desensitized optimal trajectory for landing on small bodies with reduced landing error. Aerosp. Sci. Technol. **48**, 178–185 (2016). https://doi.org/10.1016/j.ast.2015.11.006
8. Lan, Q., Li, S., Yang, J., Guo, L.: Finite-time soft landing on asteroids using nonsingular terminal sliding mode control. Trans. Inst. Measur. Control **36**(2), 216–223 (2014). https://doi.org/10.1177/0142331213495040

9. Li, S., Cui, P., Cui, H.: Autonomous navigation and guidance for landing on asteroids. Aerosp. Sci. Technol. **10**(3), 239–247 (2006). https://doi.org/10.1016/j.ast.2005.12.003
10. Lunghi, P., Lavagna, M., Armellin, R.: A semi-analytical guidance algorithm for autonomous landing. Adv. Space Res. **55**(11), 2719–2738 (2015). https://doi.org/10.1016/j.asr.2015.02.022
11. Mao, Y., Szmuk, M., Açıkmeşe, B.: Successive convexification of non-convex optimal control problems and its convergence properties. In: 2016 IEEE 55th Conference on Decision and Control (CDC), pp. 3636–3641. IEEE (2016)
12. Pinson, R.M., Lu, P.: Trajectory design employing convex optimization for landing on irregularly shaped asteroids. J. Guid. Control Dyn. **41**(6), 1243–1256 (2018). https://doi.org/10.2514/1.G003045
13. Werner, R.A., Scheeres, D.J.: Exterior gravitation of a polyhedron derived and compared with harmonic and mascon gravitation representations of asteroid 4769 castalia. Celestial Mech. Dyn. Astron. **65**(3), 313–344 (1996)
14. Stephen P., Lieven, V.: Convex Optimization. In: Cambridge University Press (2004)
15. Szmuk, M., Acikmese, B.: Successive convexification for 6-dof mars rocket powered landing with free-final-time. In: 2018 AIAA Guidance, Navigation, and Control Conference, p. 0617 (2018). https://doi.org/10.2514/6.2018-0617
16. Szmuk, M., Acikmese, B., Berning, A.W.: Successive convexification for fuel-optimal powered landing with aerodynamic drag and non-convex constraints. In: AIAA Guidance, Navigation, and Control Conference, p. 0378 (2016). https://doi.org/10.2514/6.2016-0378
17. Yang, H., Bai, X., Baoyin, H.: Finite-time control for asteroid hovering and landing via terminal sliding-mode guidance. Acta Astronaut. **132**, 78–89 (2017). https://doi.org/10.1016/j.actaastro.2016.12.012
18. Yang, H., Bai, X., Baoyin, H.: Rapid generation of time-optimal trajectories for asteroid landing via convex optimization. J. Guid. Control Dyn. **40**(3), 628–641 (2017). https://doi.org/10.2514/1.G002170
19. Yang, H., Bai, X., Baoyin, H.: Rapid trajectory planning for asteroid landing with thrust magnitude constraint. J. Guid. Control Dyn. **40**(10), 2713–2720 (2017). https://doi.org/10.2514/1.G002346
20. Yang, H., Baoyin, H.: Fuel-optimal control for soft landing on an irregular asteroid. IEEE Trans. Aerosp. Electron. Syst. **51**(3), 1688–1697 (2015). https://doi.org/10.1109/TAES.2015.140295
21. Zexu, Z., Weidong, W., Litao, L., Xiangyu, H., Hutao, C., Shuang, L., Pingyuan, C.: Robust sliding mode guidance and control for soft landing on small bodies. J. Franklin Inst. **349**(2), 493–509 (2012). https://doi.org/10.1016/j.jfranklin.2011.07.007